NONDESTRUCTIVE CHARACTERIZATION OF CERAMIC COMPOSITE WHISKERS WITH NEUTRON DIFFRACTION AND ULTRASONIC TECHNIQUES*

D. S. Kupperman, S. Majumdar, S. R. MacEwen,**
R. L. Hitterman†, J. P. Singh, R. A. Roberts,
and J. L. Routbort,†

Materials and Components Technology Division
Argonne National Laboratory
9700 South Cass Avenue
Argonne, Illinois 60439

INTRODUCTION

A necessary step in the development of structural composites is the understanding and characterization of the bond between fiber and matrix. Questions regarding the mechanical properties of the optimum interfacial bond and how properties of the bond can be assessed nondestructively must be answered. In this paper we present some results of a program at Argonne National Laboratory (ANL) in which the characterization and control of interfacial bonds in composites are being investigated. The General Purpose Powder Diffractometer (GPPD) at the Intense Pulsed Neutron Source (IPNS) at ANL has been employed to measure residual strains in a ceramic-ceramic composite by neutron diffraction techniques. From the residual strain measurements it is possible to calculate stresses at the fiber-matrix interface. The results of the residual strain experiment and the initial results from experiments in which ultrasonic techniques were used to assess whisker-matrix bonding are discussed in this paper.

APPLICATION OF NEUTRON DIFFRACTION TECHNIQUES TO MEASUREMENT OF RESIDUAL STRAIN IN Al_2O_3/SiC

Specimen

The sample used in this study, supplied by ARCO [1], was a composite composed of an alumina (Al_2O_3) matrix with silicon carbide (SiC) whiskers (15% by weight). The SiC whiskers, blended with Al_2O_3 and hot-pressed into samples 30 x 25 x 5 mm thick, are ~10-30 μm long and 0.75 μm in

*This work has benefitted from the use of the Intense Pulsed Neutron Source at Argonne National Laboratory which is funded by the U.S. Department of Energy, BES-Materials Science, under Contract. No. W-31-109-ENG-38.

**Chalk River Nuclear Laboratories, Advanced Materials Research Science Branch, Chalk River, Ontario, Canada.

†Materials Science Division, Argonne National Laboratory, Argonne, IL.

diameter. The whiskers have a high defect density, primarily due to stacking faults, and their crystallographic structure is not clearly defined [2]. Although reference to the alpha (hexagonal) form can be found in the literature [3], some predominant neutron (and X-ray) diffraction peaks associated with the alpha form are absent, and all primary peaks for the beta (cubic) form are clearly present. As a result, in order to carry out the strain and stress analysis, we assume the cubic structure. This assumption should not result in serious analytical errors as the (111) and (220) planes of the cubic structure have the same lattice spacing as the (002) and (110) planes of the hexagonal structure, and the <111> direction of the cubic structure and <002> of the hexagonal structure are both parallel to the whisker axis.

Although the whiskers are randomly distributed in the powder before pressing, the hot-pressing process results in some texturing [3] because few whiskers are oriented with the long axis parallel to the pressing direction. A micrograph of a fracture surface from a slice of this sample (Fig. 1) shows the whiskers and Al_2O_3 grains and clearly indicates fiber pull-out. The pressing direction is from top to bottom. In order to carry out the neutron diffraction experiment, the sample was cut into two 30 x 10 x 5 mm-thick pieces to partially fill a vanadium tube 10 mm in diameter and 60 mm high. The pressing direction was aligned parallel to the incident n-beam.

Fig. 1. Micrograph of Al_2O_3/SiC sample showing SiC whiskers.

Neutron Diffraction

Although it will be clear from the following discussion that, at present, neutron diffraction cannot be used on a routine basis for non-destructive evaluation (NDE), it is a powerful method for measuring bulk residual strains from which residual stresses can be calculated. The technique can be used to study fabrication processes, validate or calibrate other techniques for measurement of stress (e.g. ultrasonic techniques), or confirm the validity of model calculations. In the wavelengths of interest for stress measurement, neutrons can penetrate deeper than x-rays and thus can provide a bulk measurement. Neutrons can also be used to measure stress in a sample as a function of position, thus providing information on stress gradients.

Thermal neutrons with velocities of up to 1000 m/s are of interest for neutron diffraction. At these energies, the wavelengths are on the order of the lattice spacing, allowing application of Bragg's Law of diffraction to neutrons as

$$2d_{hkl} \sin \theta = \lambda_{hkl} \quad ,$$

where d is the lattice spacing, 2θ is the angle between incident and scattered neutron beams when a Bragg peak is detected, λ is the de Broglie wavelength of the neutron, and h, k, and l are the Miller indices of the diffracting plane. In the experiments described here, Bragg's law is used first to determine lattice spacings d for particular hkl reflections from both Al_2O_3 and SiC averaged over a volume of the strain-free powder. Next, the stressed composite is examined. The lattice strain associated with the hkl plane of a given phase in the composite is given by $e = (d - d_o)/d_o$, where d_o is the unstrained hkl spacing in the powder and d is the spacing in the composite. If the samples are examined with a monochromatic beam, $e = -\cot \theta \, (\Delta\theta)$, where $\Delta\theta$ is the small change in Bragg angle between the samples for wavelength λ. If the samples are placed in a pulsed beam of "white" neutrons, as is done here with the ANL IPNS, the Bragg diffraction peak is observed at a fixed scattering angle $\Phi = 2\theta$, and

$$\theta = \Delta\lambda/\lambda = \Delta t/t \quad ,$$

where $t = L\lambda m/h$ is the time for the neutron of mass m to travel a distance L, and h is Planck's constant [4]. The main advantage of the pulsed source is that many diffraction peaks can be measured at the same time. The neutron pulses are generated at ANL by accelerating protons to a very high energy (500 Mev) and directing them at a uranium target. The fast neutrons created by spallation are moderated and produce beams at various instruments such as the GPPD used for powder diffraction experiments. The pulse repetition rate is 30 cycles/s with a peak thermal flux of about 4×10^{14} neutrons/cm^2. The GPPD, with a resolution that is almost independent of d-spacing (about 0.25% for 148°), is about 20 m from the target. Neutrons are detected with banks of ^{3}He proportional counters (140 total) encircling the sample chamber on a 1.5 m scattered flight path, at 20°, 30°, ±60°, ±90° and ±148° relative to the neutron forward direction. Data are collected by a PDP 11/34-Z8000 computer.

For SiC, the diffraction peaks of principal interest are the (111) and (220) since the <111> and <220> crystallographic directions are parallel and perpendicular to the SiC whisker axes, respectively. In principle, the stresses in the whisker could be calculated from the residual strains in these directions. However, although residual strains are well defined, there are complications in the analysis which make it difficult to define the whisker stresses precisely.

Thermal Expansion Coefficients and Temperature Dependent Measurement of Residual Strain

Cooling the hot-pressed composite after forming could cause high residual compressive stresses in the whiskers due to differential thermal contraction. From 0 to 1000°C, the thermal expansion of Al_2O_3 is 8.8 x $10^{-6}°C^{-1}$, and that of SiC is 4.7 x $10^{-6}°C^{-1}$[5]. Lattice expansion and residual strains were measured at temperatures from 25 to 1000°C in a furnace specially designed for the GPPD. The sample was encapsulated in a vanadium tube and held at each temperature for two hours to acquire enough neutron counts. Figure 2 shows the expansion of the lattice spacing versus temperature for various Al_2O_3 and SiC crystallographic planes in the powder and the hot pressed composite. A comparison of the results obtained from the powder with those obtained from the composite indicates that, in the hot-pressed sample, the axial stresses in the SiC, on the average, are substantially higher than the axial stresses of the Al_2O_3. This is the result of the higher stiffness and lower volume fraction of the SiC (radial stresses of the Al_2O_3 and SiC are equal at the interface). As the temperature is raised (relaxing the thermally induced stress), the SiC lattice spacing increases much faster in the composite than in the powder, showing that the whiskers were under substantial stress. The thermal expansion coefficients, α, of Al_2O_3 and SiC, calculated from the data of Fig. 2, are close to that in Ref. 5. Table 1 shows representative values of mean thermal expansion coefficients for several crystallographic directions in the temperature range 25-1000°C.

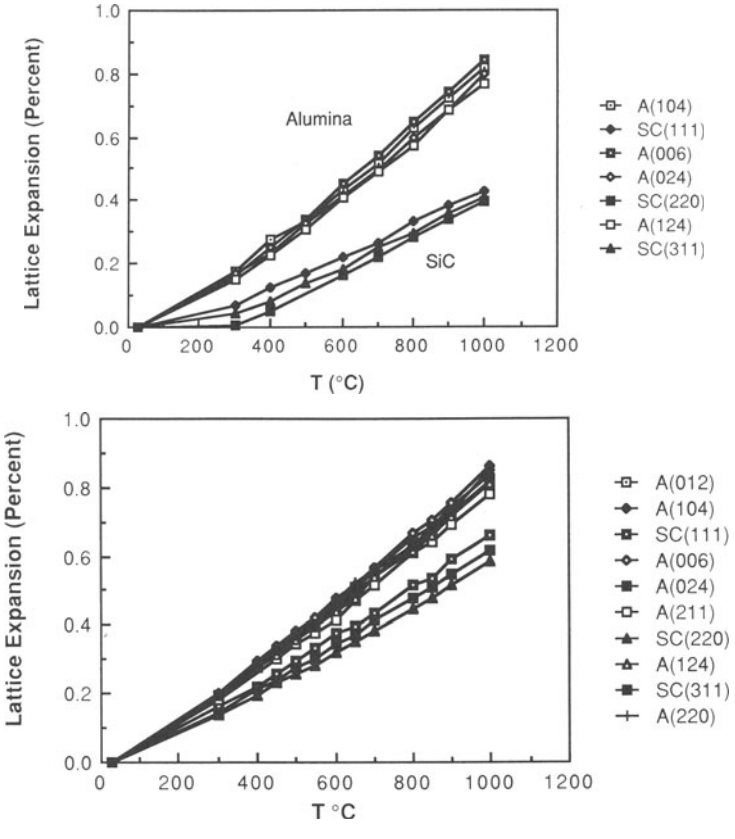

Fig. 2. Lattice expansion of various Al_2O_3 and SiC planes for powder (top) and hot-pressed (lower) samples. In the figure legend, A = Al_2O_3 and SC = silicon carbide.

Table 1. Mean Thermal Expansion Coefficients of Al_2O_3 and SiC at 25-1000°C ($\mu m/\mu m$ °C x 10^6)

Al_2O_3		SiC	
(hkl)	(α)	(hkl)	(α)
(104)	8.5	(111)	4.5
(006)	8.6	(220)	4.2
(024)	9.1	(311)	4.3
(221)	7.8	(422)	5.5
Average	8.3		4.6

Residual strains obtained from the differences in lattice spacing data between hot-pressed and powder samples for various crystallographic directions in SiC and Al_2O_3 are shown in Fig. 3. Again it is clear that the magnitude of the strains, and thus the stresses, in the SiC whiskers is much larger than in the Al_2O_3 matrix (up to 0.32%). Furthermore, the strains asymptotically approach 0 as the stresses are relieved by thermal expansion. The strain appears to be totally relieved at 1300-1400°C. This is consistent with the idea that, on cooling from hot pressing, strain starts to build up significantly a few hundred degrees below the fabrication temperature of about 1700°C. That is, above ~1400°C, the stresses are relieved by creep mechanisms.

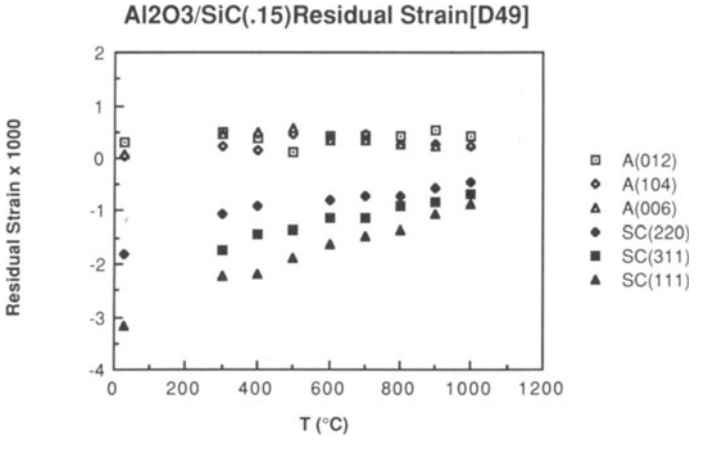

Fig. 3. Residual strain vs. temperature for various planes of Al_2O_3/SiC.

Comparison of Residual Strain Data to Model Calculations

The strains and stresses in the fiber were calculated theoretically by a modified Eshelby model [6], in which ellipsoidal fibers with elastic bulk modulus K_1 and shear modulus μ_1 are embedded in an elastic matrix with bulk modulus K and shear modulus μ. A self-consistent approach is used, so that each fiber is assumed to be embedded in a composite with average bulk and shear modulii $\langle K \rangle$ and $\langle \mu \rangle$. The average properties are also determined from the model. For the purpose of this paper, the whiskers, which are approximated by prolate spheroids with a length to diameter ratio of 16, are assumed to be distributed randomly, both in orientation and location, in the composite. The stress analysis is conducted in the local fiber coordinates, axial $x_1\langle 111 \rangle$, radial $x_2\langle 110 \rangle$, and tangential $x_3\langle 112 \rangle$. In reality, the fibers are transversely isotropic in the x_2-x_3 plane, so that the elastic constants and coefficients of thermal expansion in the fiber axis direction (111) are different from those in the transverse directions. To apply Eshelby's model, the anisotropic elastic constants [7] are replaced by average isotropic elastic constants. However, once the transformation strains are obtained, the transversely isotropic constants are used to compute the stresses in the fiber. Stresses and strains in any other direction are obtained by tensor transformation. The details of the stress analyses are given in Ref. 8. Figure 4 shows the predicted and observed strains for the various crystallographic directions. The calculations, at a minimum, are expected to be within the bounds of the experimental results, which are a texture-weighted average. Good agreement is seen for the $\langle 110 \rangle$ directions which are perpendicular to the whisker axis. Comparison of predicted with observed strains for the $\langle 111 \rangle$ direction shows strains less than predicted along the whisker axis. If fiber slippage is present, the experimental data should be lower than predicted by model calculation. It is possible that observed strains have been relieved by slippage during cooling after hot-pressing. If this is the case, residual strain measurements could provide information about the bond quality and the forces acting at the whisker-matrix boundary. Further efforts will be needed to confirm this speculation. Calculations of stress and comparisons to theory are more difficult because of the anisotropy due to the pressing process and the lack of clear crystallographic structure. A future publication [8] will address the issue of calculating and predicting stresses in the whiskers.

Ultrasonic Velocity Data and Comparison to Model Calculations

Ultrasonic velocities were measured in Al_2O_3/SiC and Si_3N_4/SiC composites. Pulse overlap techniques at 20 MHz were carried out by means of a normal-incidence shear-wave transducer. A comparison of the variation of experimentally determined velocity variation with SiC volume fraction to model predictions may provide a qualitative assessment of interfacial-bond quality. For example, an analysis of scanning electron microscopy images of fracture surfaces and comparison of velocity data to expected values for perfect interfacial bonding (Voigt and Reuss limits, [9]) indicate that transverse sound velocities may be useful in characterizing interfacial-bond strength [10] by observing differences between model predictions and experimental results. The shear velocities measured in Si_3N_4/SiC, where almost perfect bonding is present, are close to the Reuss lower bound. On the other hand, the shear velocities in the Al_2O_3/SiC, where imperfect bonding (the result of a glassy phase) is probable, are significantly below the Reuss limit. Fig. 5 shows the results.

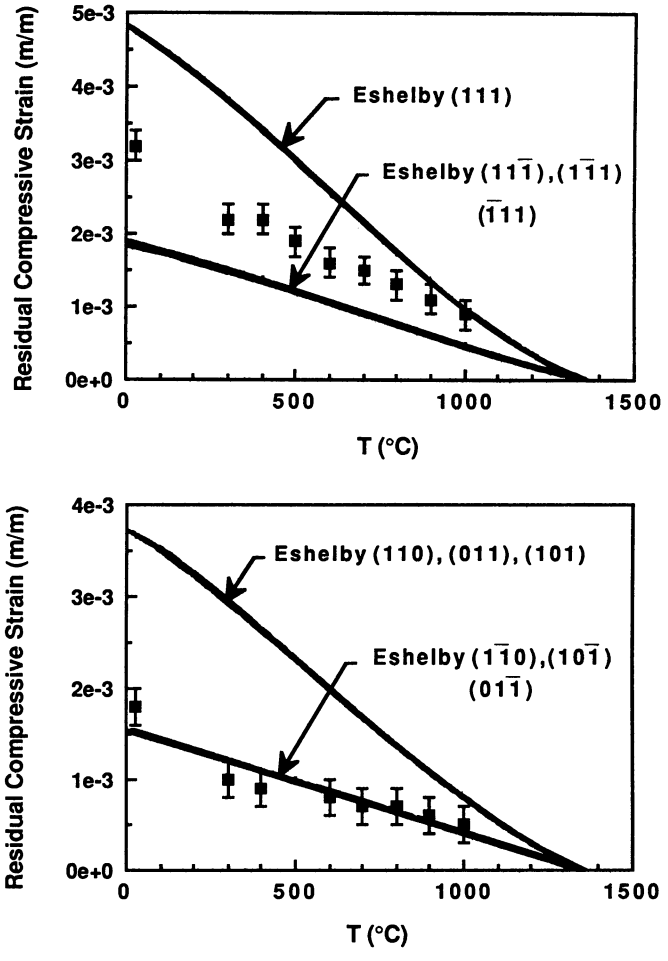

Fig. 4. Predicted vs. observed strain in SiC whiskers of Al_2O_3/SiC.

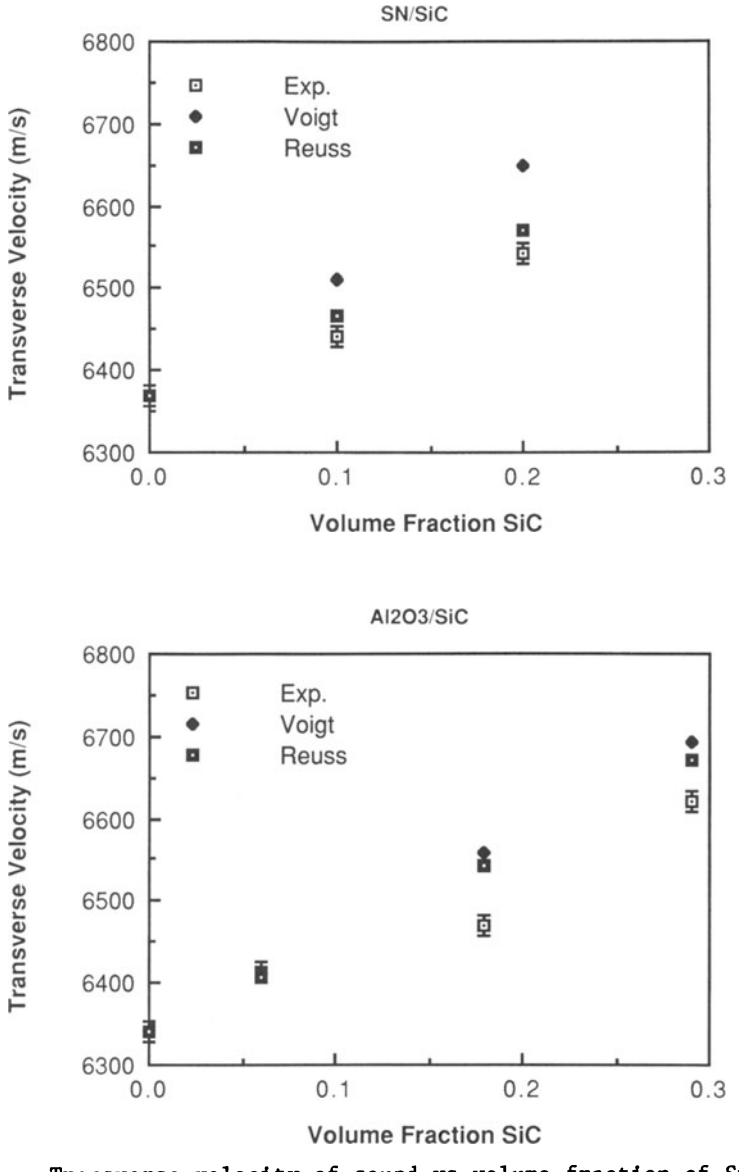

Fig. 5. Transverse velocity of sound vs volume fraction of SiC for Si_3N_4/SiC and Al_2O_3/SiC composites. In the figure legend, SN = silicon nitride.

REFERENCES

1. ARCO Chemical Co., Greer, SC (courtesy J. Rhodes).

2. S. R. Nutt, J. Am. Ceram. Soc. 67(6), June 1984.

3. J. R. Porter, F. F. Lange, and A. H. Chokshi, Am. Ceram. Soc. Bull. 66(2), 343-47 (1987).

4. A. J. Allen, M. T. Hutchings, C. G. Windsor, and C. Andreani, in Advances in Physics, 1985, Vol. 34, No. 4, p. 445-473.

5. W. D. Kingery, H. K. Bowen and D. R. Uhlmann, Introduction to Ceramics, Wiley and Sons, New York, 1975, p. 595.

6. J.D. Eshelby, Proc. R. Soc. Edinburgh, Sect. A, 241, 376-396 (1957).

7. K. B. Tolpygo, Sov. Phys. Solid State, 2, 2367 (1961).

8. S. Majumdar, et al., unpublished results.

9. S. Lees and C. L. Davidson, IEEE Trans. Sonics and Ultrason. SU-24(3), (1975).

10. A. K. Mal and S. K. Bose, Proc. Cambridge. Philos. Soc. 76, 587 (1974).